Confinement and correlation effects on plasmons in an atom-scale metallic wire

2010 J. Phys.: Condens. Matter 22 135003

(http://iopscience.iop.org/0953-8984/22/13/135003)

J. Phys.: Condens. Matter **22** (2010) 135003 (6pp) doi:10.1088/0953-8984/22/13/135003

Confinement and correlation effects on plasmons in an atom-scale metallic wire

R K Moudgil[1], Vinayak Garg[2] and K N Pathak[3]

[1] Department of Physics, Kurukshetra University, Kurukshetra-136 119, India
[2] Department of Physics, Punjabi University, Patiala-147 002, India
[3] Department of Physics, Center for Advanced Study in Physics, Panjab University, Chandigarh-160 014, India

E-mail: rkmoudgil13@gmail.com

Received 17 November 2009, in final form 25 January 2010
Published 25 February 2010
Online at stacks.iop.org/JPhysCM/22/135003

Abstract
We have studied the effect of confinement and correlations on the plasmon dispersion in an atom-scale metallic wire by determining the electron density response function. The wire electrons are modelled as comprising a quasi-one-dimensional homogeneous gas, with different transverse confinement models. The response function is calculated by including electron correlations beyond the random-phase approximation within the self-consistent mean-field approach of Singwi *et al* (1968 *Phys. Rev.* **176** 589). The plasmon dispersion results are found to be in very good agreement with the recent electron-energy-loss spectroscopy measurements by Nagao *et al* (2006 *Phys. Rev. Lett.* **97** 116802). However, our predictions are found to depend strongly on the nature of the confinement model, the structure of the one-dimensional electronic band and the electron effective mass, implying a crucial role for the wire structure.

1. Introduction

The study of elementary electronic excitations in one-dimensional (1D) electron systems has generated considerable theoretical [1–7] as well as experimental [8–13] interest during the last two decades. Here, the electrons are free to move in one direction whereas their transverse motion is restricted quantum mechanically. Advances in material fabrication technology at the nano-scale have enabled the realization of 1D electron channels with a very fine control on the system parameters. The early [14] 1D electron systems were tailored by providing confinement to electrons along one of the two lateral directions in a two-dimensional (2D) electron gas formed at the interface of a semiconductor quantum-well structure; for example, the AlGaAs–GaAs–AlGaAs quantum well. In this way, 1D electron channels with (lateral) width of the order of 100 nm were created. At the experimentally accessible in-plane electron densities, however, the electrons occupied the higher energy subbands along the confinement direction. The excitation spectrum of such electron systems has been measured through inelastic light scattering experiments [9], which have confirmed the theoretical prediction [3, 4] of the excitation of both the intra- and inter-subband plasmons. Rather, quantitative agreement is found with a theoretical calculation based on the random-phase approximation (RPA). This agreement is quite understandable, as the experimental wire parameters correspond to a weakly coupled 1D electron system and therefore correlation effects are not expected to be significant.

However, recently, narrower 1D electron channels (∼nm) have been realized in atomic-scale metallic quantum wires [15–19] grown on a semiconductor surface. Among these, a single chain of Au atoms anchored rigidly to a step on a highly stepped Si(557)–Au surface has attracted much attention. Due to reduced channel width, the chain electrons are expected to occupy only the lowest energy subband for their transverse motion, and consequently they are believed to map almost exactly a 1D electron system [11, 12]. But angle-resolved photoemission experiments [16, 17] have revealed a non-trivial electronic band structure of the Au chain, particularly the splitting of the 1D conduction band into two peaks near the Fermi level. Right from its realization, this electron system has been providing interesting puzzles like the assignment [15] of band splitting to the Luttinger liquid [20] behaviour of 1D electrons (i.e. the spin–charge separation), metallic behaviour [17] despite an even number of electrons per unit cell, a metal–insulator transition [12, 18] with lowering of temperature, etc. However, recent *ab initio* calculations [21]

have shown that it is the spin–orbit (SO) coupling that causes splitting of the conduction band into the two 1D bands, thus ruling out the reported manifestation [15] of spin–charge separation. Very recently, Nagao *et al* [11, 12] have measured the plasmon dispersion in the Au chain on the Si(557)–Au surface by using electron-energy-loss spectroscopy. The measured plasmon has been found to exhibit 1D and metallic characteristics. Motivated directly by these measurements, we present[4] in this work a theoretical calculation of plasmon excitation energy for the Au metallic wire. We employ the dielectric formulation [22] wherein the poles of the density–density response function yield the plasmon excitation energy. The density response function is calculated within the framework of the generalized self-consistent mean-field approximation. We specifically investigate the dependence of plasmon energy on the nature of transverse confinement, electron correlations and structure of the 1D electronic band. Our results are compared directly with the experimental data of Nagao *et al* [11].

The rest of the paper is organized as follows: in section 2, the wire model is presented with special emphasis on the effect of the confinement model on the effective electron–electron (e–e) interaction potential. Section 3 contains a brief account of the theoretical formalism. The results and discussion are presented in section 4. The paper is concluded in section 5.

2. Wire model

The x-ray diffraction study of the stepped Si(557)–Au surface by Robinson *et al* [19] has revealed (see figure 3 of [19]) that each terrace on the Si surface has a width of ∼1.9 nm and holds a single Au chain in its middle, along with the adatom (Si) row and the step edge. However, we ignore here the inter-chain coupling as the inter-chain spacing is about four times the average intra-chain electron separation ($\sim a_0^*$ is the effective Bohr atomic radius). According to recent *ab initio* calculations [21], the electronic band associated with the Au chain develops appreciable (∼0.3 eV) SO-splitting near the Fermi level, and both the bands are metallic. In contrast, Ahn *et al* [18] have deduced through angle-resolved photoemission measurements that only one band is metallic at room temperature. In our study, we shall consider both the single- and two-metallic band situations.

We model the Au chain as a quasi-1D homogeneous gas of electrons (with band effective mass m^*) embedded in a rigid positive charge background to maintain electrical neutrality. The motion of electrons is free along the wire axis (say the x axis) while it is confined quantum mechanically in the transverse plane (i.e. the y–z plane). Realizing that the wire has finite width, we assume that the transverse motion is confined by a 2D potential $V_c(y, z)$ symmetric about the x axis. The confinement is supposed to be sufficiently strong that the electrons occupy only the lowest energy subband for the transverse motion. The one-electron wavefunction is then of the form

$$\psi(x, \mathbf{R}) = L^{-1/2}\, \mathrm{e}^{\imath qx}\phi(\mathbf{R}), \tag{1}$$

where L denotes the wire length and $\phi(\mathbf{R})$ the transverse part of the total wavefunction ($\mathbf{R} \equiv y, z$). Accordingly, the Fourier transform of the effective e–e interaction potential is given by

$$V(q) = \frac{e^2}{\epsilon_0}\int_{-\infty}^{\infty} \mathrm{d}(x - x')\mathrm{e}^{\imath q(x-x')} \times \int\int \mathrm{d}\mathbf{R}\,\mathrm{d}\mathbf{R}' \frac{|\phi(\mathbf{R})|^2|\phi(\mathbf{R}')|^2}{\sqrt{(x-x')^2 + (|\mathbf{R}-\mathbf{R}'|)^2}}, \tag{2}$$

with ϵ_0 being the dielectric constant of the substrate material. To see the role of the nature of confinement, we consider some different confinement models developed in literature.

(I) Harmonic confinement in the y–z plane [1]: here, $V_c(R) = \hbar^2 R^2/(8m^* b^4)$, with b being the wire width; hereafter, we chose a system of units in which $\hbar = 1$. In the lowest energy subband, $\phi(R) = (2\pi b^2)^{-1/2}\exp(-R^2/4b^2)$, and the integral (2) is evaluated analytically to give $V(q)$ as

$$V(q) = \frac{e^2}{\epsilon_0}\exp(q^2b^2)E_1(q^2b^2), \tag{3}$$

where $E_1(x)$ is the exponential–integral function.

(II) Infinite square-well confinement in the y–z plane [23]: in this case, $V(q)$ has to be obtained numerically as

$$V(q) = \frac{2e^2}{\epsilon_0}\int_0^a \mathrm{d}y\int_0^a \mathrm{d}y'\int_0^a \mathrm{d}z\int_0^a \mathrm{d}z'\,|\phi(y,z)|^2 \times |\phi(y',z')|^2 K_0(q\sqrt{(y-y')^2 + (z-z')^2}), \tag{4}$$

with $\phi(y, z) = (2/a)\sin(\pi y/a)\sin(\pi z/a)$, $K_0(x)$ the zeroth-order modified Bessel function of the second kind, and a the width of the square well.

(III) Infinite square-well confinement in the y direction and an optimized wavefunction $\zeta(z)$ in the z direction [2]: now, $\phi(y, z) = (2/a)^{1/2}\sin(\pi y/a)\zeta(z)$ in integral (4), with z integral from 0 to ∞; $\zeta(z) = (\beta^3/2)^{1/2} z\exp(-\beta z/2)$, with $\beta = 3/\langle z_0\rangle$ being a variational parameter and $\langle z_0\rangle$ the average wire width along the z direction. This form of $\zeta(z)$ was originally used by Stern and Howard [24] to describe the width of a 2D electron gas in a semiconductor quantum well.

(IV) Harmonic confinement in the y direction and $\sqrt{\delta(z)}$ wavefunction in the z direction [25]: for this model, $V(q)$ can be obtained analytically as

$$V(q) = \frac{e^2}{\epsilon_0}\exp(q^2b^2/4)K_0(q^2b^2/4). \tag{5}$$

(V) Infinite square-well confinement in the y direction and $\sqrt{\delta(z)}$ wavefunction in the z direction [3]: in this case, $V(q)$ is given by

$$V(q) = \frac{8e^2}{\epsilon_0 a^2}\int_0^a \mathrm{d}y\int_0^a \mathrm{d}y'\sin^2(\pi y/a) \times \sin^2(\pi y'/a)K_0(q|y-y'|). \tag{6}$$

[4] Very preliminary results on electron interaction potential and plasmon excitations were submitted for presentation at the 54th DAE Solid State Physics Symposium held at M S University of Baroda (India) in December 2009.

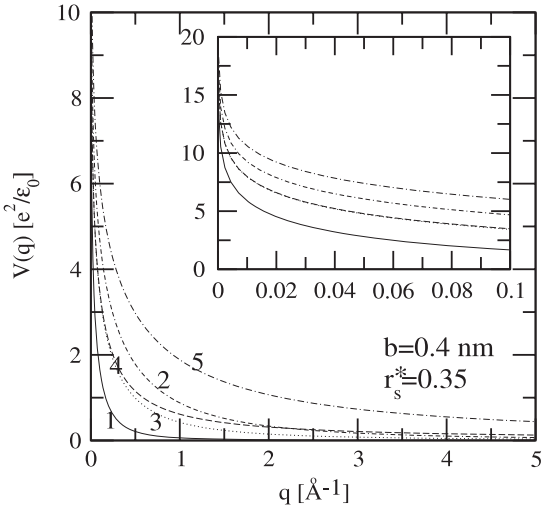

Figure 1. The effective electron–electron interaction potential $V(q)$ versus wavenumber q for different confinement models. The curves labelled as 1, 2, 3, 4 and 5 correspond, respectively, to the five confinement models described in the text. The inset depicts $V(q)$ in the small q region with curves labelled in the same way as in the main panel; the results of models III and IV are almost indistinguishable.

In figure 1, we compare $V(q)$ for the above confinement models by taking $b = 0.4$ nm and $r_s^* = 0.35$; r_s^* is the (effective) coupling parameter which is related to the linear electron number density n as $r_s^* = 1/(2na_0^*)$, with $a_0^* = \epsilon_0/(m^*e^2)$. The square-well width a (in models II, III and V) and the average width $\langle z_0 \rangle$ (in model III) are taken to be equal to b. Evidently, $V(q)$ depends strongly on the nature of the confinement potential. The square-well confinement results in somewhat harder e–e interaction compared to the harmonic case. Also, taking a $\sqrt{\delta(z)}$-type wavefunction, which is equivalent to the assumption of zero wire width in the z direction, results in a much harder interaction potential. Further, it is clear from the inset of figure 1 that $V(q)$ has significant dependence on the confinement model over the wavevector range that is currently accessible to inelastic scattering experiments. This indicates that the choice of confinement model may depend on the fabricated 1D structure and it should be crucial in the theoretical description of the electronic properties of quantum wires. Its effect on plasmon dispersion shall be examined in section 4.

Although Nagao *et al* [11] have measured plasmon dispersion at room temperature, we assume here that the electron system is at absolute zero temperature. This assumption seems to be quite reasonable, as for the Au chain $k_BT/E_F \sim O(10^{-2})$ at $T = 300$ K; E_F is the 1D Fermi energy. Under these conditions, the wire model is characterized completely by the coupling parameter r_s^* and the wire width b.

3. Theoretical formalism

We use the dielectric formulation, where the density response function $\chi(q, \omega)$ (which describes the response of electrons to a weak space–time dependent external longitudinal electric potential) constitutes a quantity of central importance. The poles of $\chi(q, \omega)$ yield directly the plasmon excitation energy. However, the many-body nature of the system forbids exact calculation of $\chi(q, \omega)$. We determine $\chi(q, \omega)$ by employing the generalized mean-field approximation [22] (within the linear response framework) and $\chi(q, \omega)$ is given as

$$\chi(q, \omega) = \frac{\chi_0(q, \omega)}{1 - V(q)[1 - G(q)]\chi_0(q, \omega)}, \tag{7}$$

where

$$\chi_0(q, \omega) = \frac{m^* g_s}{2\pi q} \ln\left\{\frac{\omega^2 - (qk_F/m^* - q^2/2m^*)^2}{\omega^2 - (qk_F/m^* + q^2/2m^*)^2}\right\}, \tag{8}$$

is the (zero temperature) free electron density response function (the so-called 1D Lindhard function) and $G(q)$ is the local-field correction (LFC) factor, which describes the modification of $V(q)$ due to exchange–correlation effects. Here, g_s is the spin degeneracy factor and $k_F = \pi n/g_s$ is the 1D Fermi wavevector. Setting $G(q) = 0$ corresponds to the RPA. We use the self-consistent mean-field approximation of Singwi, Tosi, Land and Sjölander (STLS) [26] to deal with the electron correlation effects. The STLS approach, developed originally for a three-dimensional electron system [26], has been generalized in the literature to study the 2D [27] and 1D [1] electron systems. In this approach, $G(q)$ is given in terms of the static density structure factor $S(q)$ and for a quasi-1D system it is given as

$$G(q) = -\frac{1}{n}\int_{-\infty}^{\infty} \frac{dq'}{2\pi} \frac{q'V(q')}{qV(q)}[S(|\mathbf{q} - \mathbf{q}'|) - 1]. \tag{9}$$

In turn, $S(q)$ is related to the imaginary part of $\chi(q, \omega)$ through the fluctuation–dissipation theorem as

$$S(q) = -\frac{1}{\pi n}\int_0^{\infty} d\omega \, \mathrm{Im}\, \chi(q, \omega). \tag{10}$$

Evidently, the density response function $\chi(q, \omega)$ can only be determined numerically from the self-consistent solution of equations (7), (9) and (10).

The plasmon excitation energy $\omega_p(q)$ is obtained readily from the poles of equation (7) as

$$\omega_p(q) = \sqrt{\frac{\omega_-^2 - \omega_+^2 e^{A(q)}}{1 - e^{A(q)}}}, \tag{11}$$

with $A(q) = 2\pi q/[m^* g_s V(q)\{1 - G(q)\}]$ and $\omega_\pm = (q^2/2 \pm qk_F)/m^*$. $|\omega_-|$ and ω_+ correspond, respectively, to the lower and upper boundary of the (single) electron–hole pair continuum. The numerical results of $\omega_p(q)$ are given in section 4.

4. Results and discussion

The calculation of $\omega_p(q)$ requires the LFC factor $G(q)$, which is obtained numerically by solving the set of equations (7), (9) and (10) in a self-consistent manner. We accepted the solution when convergence in the results of $G(q)$ was better than 0.0001% at each q in the chosen grid of q points. To enable a direct comparison with the experimental data of

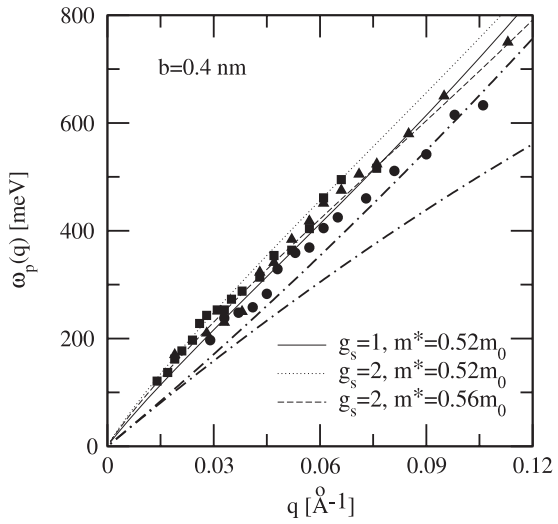

Figure 2. The plasmon energy $\omega_p(q)$ versus wavenumber q in the STLS approach at indicated wire parameters. The symbols are the experimental data of Nagao *et al* [11] for electron beams having incident energy 45 eV (■, ▲) and 35 eV (●). The thick dash–dotted lines mark the boundary of the electron–hole pair continuum at $m^* = 0.56m_0$.

Nagao *et al* [11], we use wire parameters appropriate to the Au chain on the stepped Si(557) surface: $\epsilon_0 = (1 + \epsilon_{Si})/2$, with $\epsilon_{Si} = 11.5$, $k_F = 4.1$ nm^{-1} [17] (the average of the k_F values of the two 1D bands, namely 3.8 and 4.4 nm^{-1}) and $b = 0.4$ nm. Taking the spin degeneracy parameter $g_s = 1$ corresponds to a situation where only one spin component is present in each of the two SO-split 1D bands and one of the bands is insulating. $g_s = 2$ means that both of the SO-split 1D bands are metallic and they are assumed to be degenerate, or equivalently there is no SO-splitting of the 1D band. In the latter situation, the number of active electrons is therefore exactly twice that in the former. At fixed k_F (i.e. n) and b, the calculated $\omega_p(q)$ is found to have strong dependence on the structure of the 1D band (i.e. g_s), the electron effective mass m^* and the confinement model. In our calculation, m^* is treated as a fit parameter in order to see whether a close agreement can be obtained between theory and experiment.

Figure 2 shows the $\omega_p(q)$ results for $g_s = 1$ and 2 by taking the 2D harmonic confinement model. The dispersion curve for $g_s = 1$ exhibits very good agreement with the experiment for $m^* = 0.52m_0$—a value close to $0.45m_0$ determined by photoelectron spectroscopy (PES) [17]; m_0 is the free electron mass. For this choice of m^* and g_s, $a_0^* = 0.64$ nm and $r_s^* = 0.6$. However, the corresponding $g_s = 2$ curve matches the experimental data only at small q (<0.07 Å^{-1}), and an overall good agreement is found at a somewhat higher effective mass of $0.56m_0$. But, our results for $\omega_p(q)$ are quite sensitive to the choice of confinement model (see figures 3(a) and (b)), except for models III and IV where $\omega_p(q)$ almost overlap due to the very small difference between respective $V(q)$s (see inset of figure 1). Notably, $\omega_p(q)$ shows a blue-shift as the effective e–e potential becomes harder (see figure 1) due to increased transverse confinement. One may also note that the confinement effect is relatively more pronounced for $g_s = 2$. By choosing a sufficiently larger m^*, $\omega_p(q)$ for confinement models (II–V) can also be brought closer to the experimental data. Obviously, these m^* deviate more from the PES result, with model V showing the maximum deviation; here $m^* \sim 0.8m_0$ and $0.56m_0$ for $g_s = 2$ and 1, respectively. Overall, we note that the 2D harmonic confinement model provides a reasonably good description of the transverse width of the Au chain. Our result that the best fit value of m^* for $g_s = 1$ has the minimum deviation (∼15%) from the PES experiment seems to suggest that plasmons in the Au chain correspond to one of the SO-split 1D bands. The small departure of our m^* from the PES experiment could be because of the reason that the effective mass for plasmons embodies the effect of e–e correlations in addition to the band effective mass.

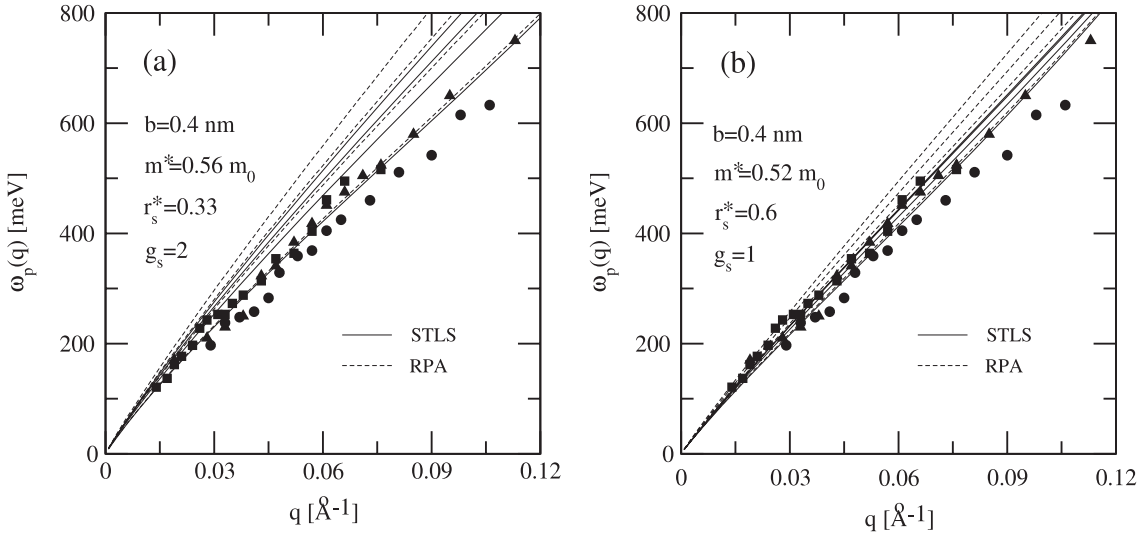

Figure 3. The dependence of the plasmon dispersion relation on the confinement model for $g_s = 2$ (in panel (a)) and 1 (in panel (b)) at indicated wire parameters in the STLS and RPA theories. The curves from bottom to top correspond to confinement models I, IV, II and V, respectively. The symbols have the same meaning as in figure 2. In panel (b), curves for models II and V overlap.

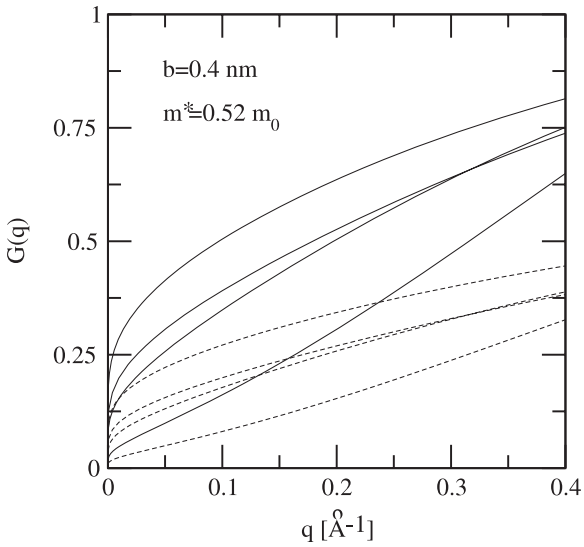

Figure 4. The local-field correction factor $G(q)$ versus wavenumber q at indicated wire parameters for different confinement models. Solid and dashed curves represent, respectively, the results for $g_s = 1$ and 2. The curves from bottom to top correspond to the confinement models I, IV, II and V, respectively.

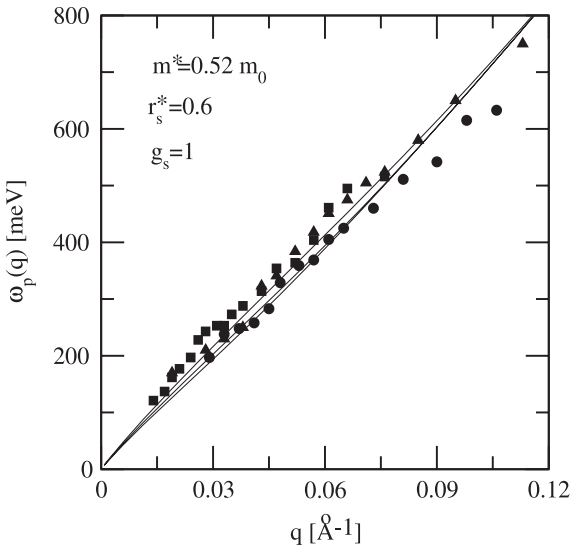

Figure 5. The dependence of the plasmon dispersion relation on the wire width b. The curves from bottom to top correspond to $b = 2$ nm, 1 nm and 0.4 nm, respectively. The symbols have the same meaning as in figure 2.

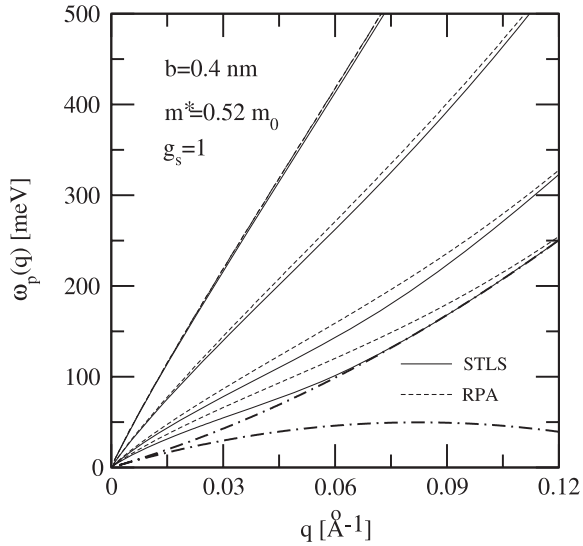

Figure 6. The dependence of the plasmon dispersion relation on the coupling parameter r_s^* at indicated wire parameters in the STLS (solid lines) and RPA (dashed lines) theories. The thick dash–dotted lines represent the boundaries of the electron–hole pair continuum at $r_s^* = 3$. The curves from bottom to top correspond to $r_s^* = 3$, 2, 1 and 0.6, respectively.

To elucidate the role of exchange–correlations, we have compared in figures 3(a) and (b) our results for $\omega_p(q)$ with the RPA. Apparently, the inclusion of correlations beyond RPA causes a red-shift in $\omega_p(q)$, and the shift increases monotonically with q. As an interesting result, the magnitude of the shift is seen to depend upon the confinement model and the g_s parameter. In particular we note that the harder the e–e interaction potential (see figure 1), the greater the red-shift in $\omega_p(q)$. In other words, the stronger the confinement, the more pronounced is the effect of exchange–correlations on $\omega_p(q)$. This result is explicitly revealed in the behaviour of the LFC factor $G(q)$, plotted in figure 4 for different confinement models. Clearly, $G(q)$ shows considerable growth with increasing confinement of the transverse motion. Also, as expected, $G(q)$ is greater for the case of $g_s = 1$. Thus, we find that depending upon the nature of confinement the exchange–correlations in 1D may become quite appreciable even though the coupling parameter r_s^* corresponds to a high density electron gas. This is an important finding of our study as the analogous 2D [28] and 3D [29] systems reveal pronounced correlations at much higher r_s^*.

In figure 5, we illustrate the dependence of $\omega_p(q)$ on the wire width b by taking $g_s = 1$, $m^* = 0.52m_0$, $k_F = 4.1$ nm^{-1} and the 2D harmonic confinement model. $\omega_p(q)$ is seen to depend weakly on b. Even by taking b as large as the width of the terrace ($\sim$1.9 nm) of the stepped Si(557) surface, $\omega_p(q)$ remains reasonably close (within the experimental error) to the experimental data. Reduction in b results in stronger confinement, and consequently $\omega_p(q)$ exhibits a mild blue-shift. Although not shown, this shift is found to be quite appreciable (particularly when $b/r_s^* < 1$) in the RPA. This difference arises due to the fact that the electron correlations, which are ignored completely in the RPA, build up with decreasing b/r_s^* and they cause a red-shift in $\omega_p(q)$, with the result that the confinement-induced blue-shift is compensated to a large extent by the correlation-induced red-shift. Qualitatively, the same reasoning explains why the STLS $\omega_p(q)$ depends weakly on the confinement model when $g_s = 1$ (see figures 3 and 4).

Although the electron density n is fixed for the Au chain, we depict in figure 6 the impact of r_s^* on $\omega_p(q)$ at $g_s = 1$, $m^* = 0.52m_0$ and $b = 0.4$ nm for the 2D harmonic confinement model. Increase in r_s^* results in suppression of $\omega_p(q)$, thus implying that less energy is required to excite a plasmon in a strongly coupled electron system. Also, comparison with the RPA shows that the exchange–correlation effects grow in strength with increasing r_s^*. Further, we note

that the plasmon excitation merges with the (single) electron–hole pair continuum (plotted for $r_s^* = 3$ in figure 6) at a critical wavevector q_c whose value decreases with the inclusion of electron correlations. However, the STLS approach (of course, the RPA also) does not account for the experimentally reported [11] damping of plasmons for $q < q_c$. Such damping may arise from the plasmon decay into two or more electron–hole pair excitations.

5. Conclusions

In conclusion, the 1D electron gas model with proper consideration of the transverse width serves as a good approximation for theoretical description of the electronic excitation spectrum of an atom-scale metallic wire. The plasmon energy $\omega_p(q)$ is found to depend strongly on the confinement model, the electron effective mass, the nature of the 1D electronic band and the coupling parameter r_s^*. The 2D harmonic confinement model is found to provide very good agreement with the experimental data of Nagao *et al*. Our study reveals that plasmons in the Au chain represent the excitation of electrons in one of the SO-split 1D energy bands. Further, we find that for the 2D harmonic model the exchange–correlation effects are not significant at experimentally accessible r_s^* and b. However, their influence grows with increasing confinement and/or increasing r_s^*/b, and they are found to cause a noticeable red-shift with respect to the RPA $\omega_p(q)$. This implies that in 1D the correlation effects may become pronounced already at smaller r_s^* values due to strong transverse confinement. Thus, our study explicitly demonstrates that the plasmons in an atom-scale metallic wire should depend on details of the wire structure. This finding may be useful in tuning of 1D plasmons, and hence in fabrication of 1D plasmonic devices.

Acknowledgment

The authors are grateful to Dr Tadaaki Nagao for sending the experimental data.

References

[1] Friesen W I and Bergersen B 1980 *J. Phys. C: Solid State Phys.* **13** 6627
[2] Das Sarma S and Lai W-Y 1985 *Phys. Rev.* B **32** 1401
[3] Li Q and Das Sarma S 1989 *Phys. Rev.* B **40** 5860
[4] Li Q P and Das Sarma S 1991 *Phys. Rev.* B **43** 11768
[5] Das Sarma S and Hwang E H 1996 *Phys. Rev.* B **54** 1936
[6] Gold A and Ghazali A 1990 *Phys. Rev.* B **41** 7626
[7] Garg V, Moudgil R K, Kumar K and Ahluwalia P K 2008 *Phys. Rev.* B **78** 045406
[8] Hansen W, Horst M, Kotthaus J P, Merkt U, Sikorski Ch and Ploog K 1987 *Phys. Rev. Lett.* **58** 2586
[9] Goñi A R, Pinczuk A, Weiner J S, Calleja J M, Dennis B S, Pfeiffer L N and West K W 1991 *Phys. Rev. Lett.* **67** 3298
[10] Demel T, Heitmann D, Grambow P and Ploog K 1988 *Phys. Rev.* B **38** 12732
Demel T, Heitmann D, Grambow P and Ploog K 1991 *Phys. Rev. Lett.* **66** 2657
[11] Nagao T, Yaginuma S, Inaoka T and Sakurai T 2006 *Phys. Rev. Lett.* **97** 116802
[12] Nagao T, Yaginuma S, Inaoka T, Sakurai T and Jeon D 2007 *J. Phys. Soc. Japan* **76** 114714
[13] Liu C, Inaoka T, Yaginuma S, Nakayama T, Aono M and Nagao T 2008 *Phys. Rev.* B **77** 205415
[14] Thornton T J, Pepper M, Ahmed H, Andrews D and Davies G J 1986 *Phys. Rev. Lett.* **56** 1198
Berggren K-F, Thornton T J, Newson D J and Pepper M 1986 *Phys. Rev. Lett.* **57** 1769
[15] Segovia P, Purdie D, Hengsberger M and Baer Y 1999 *Nature* **402** 504
[16] Losio R, Altmann K N, Kirakosian A, Lin J-L, Petrovykh D Y and Himpsel F J 2001 *Phys. Rev. Lett.* **86** 4632
[17] Altmann K N, Crain J N, Kirakosian A, Lin J-L, Petrovykh D Y, Himpsel F J and Losio R 2001 *Phys. Rev.* B **64** 035406
[18] Ahn J R, Yeom H W, Yoon H S and Lyo I-W 2003 *Phys. Rev. Lett.* **91** 196403
[19] Robinson I K, Bennett P A and Himpsel F J 2002 *Phys. Rev. Lett.* **88** 096104
[20] Tomonaga S 1950 *Prog. Theor. Phys.* **5** 544
Luttinger J M 1963 *J. Math. Phys.* **4** 1154
[21] Sánchez-Portal D, Riikonen S and Martin R M 2004 *Phys. Rev. Lett.* **93** 146803
[22] See for instance Singwi K S and Tosi M P 1981 *Solid State Phys.* **36** 177
[23] Campos V B, Degani M H and Hipólito O 1995 *Superlatt. Microstruct.* **17** 85
[24] Ando T, Fowler A B and Stern F 1982 *Rev. Mod. Phys.* **54** 437
[25] Hu G Y and O'Connell R F 1990 *Phys. Rev.* B **42** 1290
[26] Singwi K S, Tosi M P, Land R H and Sjölander A 1968 *Phys. Rev.* **176** 589
[27] Jonson M 1976 *J. Phys. C: Solid State Phys.* **9** 3055
[28] Moudgil R K, Ahluwalia P K and Pathak K N 1995 *Phys. Rev.* B **52** 11945
[29] Kumar K, Garg V and Moudgil R K 2009 *Phys. Rev.* B **79** 115304